Talanta 107 (2013) 361–367

Contents lists available at SciVerse ScienceDirect

Talanta

journal homepage: www.elsevier.com/locate/talanta

CuS nanoparticles as a mimic peroxidase for colorimetric estimation of human blood glucose level

Amit Kumar Dutta, Sudipto Das, Suvendu Samanta, Partha Kumar Samanta, Bibhutosh Adhikary, Papu Biswas *

Department of Chemistry, Bengal Engineering and Science University, Shibpur, Howrah 711103, West Bengal, India

ARTICLE INFO

Article history:
Received 29 November 2012
Received in revised form
17 January 2013
Accepted 18 January 2013
Available online 26 January 2013

Keywords:
CuS nanoparticles
Peroxidase-like activity
Hydrogen peroxide
Glucose detection
Diluted human serum

ABSTRACT

CuS nanoparticles (NPs) was synthesized through a simple and green method using water soluble precursor complex $[CuL_2(H_2O)_2]Cl_2$ (L=pyridine 2-carboxamide) and was characterized by X-ray diffraction analysis (XRD), transmission electron microscopy (TEM) and UV–Vis spectroscopic techniques. The as-prepared CuS NPs (covellite) was demonstrated to possess intrinsic peroxidase-like activity using 3,3′,5,5′-tetramethylbenzidine (TMB), as a peroxidase substrate, in presence of H_2O_2 which show good affinity towards both TMB and H_2O_2. Using this TMB–H_2O_2 catalyzed color reaction; the CuS NPs was exploited as a new type of biosensor for detection and estimation of glucose through a simple, cheap and selective colorimetric method in a linear range from 2 to 1800 μM with a detection limit of 0.12 μM. On the basis of the developed reaction process, we can easily monitor human blood glucose level.

1. Introduction

Since the first glucose sensor was proposed in 1962 [1], numerous effort has been focused on fabricating low cost and fast responsive sensors for precise monitoring of glucose levels with good selectivity, high sensitivity and reliability [2–12]. The commonly used colourimetric glucose detection method involves naturally occurring peroxidase enzyme, HRP. But HRP suffers some serious disadvantages due to lack of stability, difficult to produce in large quantities and are easily denatured in conditions like strong acidic, basic medium and high temperature. Moreover, the preparation and purification of HRP are time-consuming and expensive. Therefore, the fabrication of efficient mimics of HRP has been an increasingly important focus for the scientists and various peroxidase mimics including hematin, heme, hemoglobin, porphyrin and cyclodextrin have been investigated for this purpose [13–17]. Unfortunately, until now, there are relatively few examples of enzyme models that actually perform Michaelis–Menten catalysis under enzymatic conditions [18].

Recently, Gao et al. [19] reported that Fe_3O_4 nanoparticles (NPs) have an intrinsic enzyme mimetic activity similar to that of natural peroxidases such as horseradish peroxidase (HRP), thus opening the door for the development of nano-scaled inorganic materials in the biochemical field. Some other metal oxide, sulphide and selenide nanomaterials, such as polymer-coated CeO_2 NPs [20], CuO NPs [21,22], Co_3O_4 NPs [23], V_2O_5 nanowires [24], $BiFeO_3$ NPs [25], $CoFe_2O$ NPs [26], sheet-like FeS nanostructure [27], spherical, rod like FeS [28], CdS NPs [29], FeS and FeSe NPs [30] were also investigated and found to possess intrinsic peroxidase-like activity. Besides metal oxide nanomaterials, carbon nanomaterials including single-walled [9], helical carbon nanotubes [31], graphene oxide [10] and carbon nanodots [32] displayed intrinsic enzyme mimetic activity. These enzyme like nanomaterials could be exploited to sense immunoassay [19,20], nucleotide [9], H_2O_2 [8,10], glucose [8,10], melamine [33] and so on.

In this report, we have developed a facile and green method to fabricate CuS nanostructures and demonstrated their intrinsic peroxidase-like activity. As one of the most important transition metal chalcogenides semiconductor materials, copper sulfide (CuS), have varied applications in photocatalysis [34], solar cell devices [35], optical limiting [36], as biosensors [37] and Li-ion batteries [38]. In this paper, as a mimic peroxidase, CuS NPs exhibited good catalytic properties, stability, and dispersibility compared to other peroxidase nanomimetics and HRP. The CuS NPs were also successfully used for amperometric sensing of H_2O_2 and as peroxidase mimetics for colorimetric detection of glucose. Peroxidase has great potential for practical application and can be used as a diagnostic kit for glucose. Diabetes mellitus is one of the most common non-transmissible diseases globally, and complications that arises from it result in increasing disability, reduced life expectancy, and enormous health costs for virtually every society

* Corresponding author. Tel.: +91 332 6684561x512; fax: +91 332 6687575.
E-mail addresses: papubiswas_besus@yahoo.com, pbbesuchem@gmail.com (P. Biswas).

0039-9140/$ - see front matter © 2013 Elsevier B.V. All rights reserved.
http://dx.doi.org/10.1016/j.talanta.2013.01.032

[39]. Therefore, it is important for minimizing diabetic complications to maintain blood glucose concentrations within the normal physiological range [40]. The development of sensors for fast and reliable monitoring glucose for the diagnosis of diabetes have received continuous interest and numerous glucose sensors have been reported [11,41–48]. Among them, HRP has been widely used to fabricate sensors for detection of the products of the glucose oxidase [11,43–48]. In comparison with HRP, CuS is low-cost, easy to synthesis, much more stable to biodegradation, and not vulnerable to denaturation. These advantages show that CuS can be useful in environmental monitoring and medical diagnostics. Recently, Zhi Zheng and his co-workers [49] reported intrinsic peroxidase-like activity of CuS nanostructure but its application as amperometric biosensor for H_2O_2 and in colorimetric glucose detection yet not reported. In this paper, using CuS peroxidase-like catalytic activity and glucose oxidase (GOx), a colorimetric method for glucose detection has been developed. The results obtained indicate that this method is simple, cheap, and highly responsive and selective for glucose detection.

2. Materials and methods

2.1. Chemicals and materials

$CuCl_2 \cdot 6H_2O$, ammonia, $Na_2HPO_4 \cdot 2H_2O$, anhydrous sodium acetate, acetic acid, orthophosphoric acid, terephthalic acid and NaOH were purchased from commercial sources. 2-cyano pyridine, hydrogen peroxide (H_2O_2, 30%), dimethyl sulfoxide (DMSO), 3,3′,5,5′-tetramethyibenzidine (TMB), glucose oxidase (Aspergillus niger, GOx), β-D-glucose, maltose, α-lactose and D-fructose were purchased from Sigma-Aldrich. The blood sample was collected from a normal healthy male volunteer, then it was centrifuged and the corresponding supernatant serum was subsequently used after 2.4 times dilution with phosphate buffer solution (PBS) to reduce the matrix complexity. All other chemicals were of analytical reagent grade and used without further purification. De-ionized water was used throughout the experiment.

2.2. Preparation of CuS NPs

To a stirred solution of the precursor complex $[CuL_2(H_2O)_2]Cl_2$ (see supplementary materials) (5 mmol, 2.07 g) in 50 mL water, 0.76 g (10 mmol) thiourea in 20 mL water was added drop-wise. Then pH of the solution was adjusted to 8.0 by slowly addition of dilute ammonia. Next another 1.22 g (10 mmol) ligand, pyridine 2-carboxamide, was added to this resulting solution. The solution was then refluxed for 4 h. A greenish-black precipitate of CuS NPs was obtained. It was separated from the reaction mixture by centrifugation, washed with methanol and water for several times. The product was then dried in an air oven and kept for further characterization.

2.3. Apparatus

Elemental (C, H and N) analyses were performed on a Perkin-Elmer 2400II elemental analyzer. ^{1}H NMR spectra were recorded on a Bruker Avance DPX spectrometer at 300 MHz. Powder XRD patterns were obtained on a Philips PW 1140 parallel beam X-ray diffractometer with Bragg–Bretano focusing geometry and monochromatic CuKα radiation (λ=1.540598 Å). TEM measurements were made on a JEOL JEM-2100 microscope using an accelerating voltage of 200 kV. FT-IR spectra were recorded using KBr disks on a JASCO FTIR-460 plus spectrophotometer. Colorimetric glucose detection process and peroxidase-like activity were performed spectrophotometrically using Agilent-8453 diode-array spectrophotometer.

2.4. Peroxidase-like activity measurements

The peroxidase-like activity of the CuS NPs was investigated through the catalytic oxidation of the peroxidase substrate 3,3′,5,5′-tetramethylbenzidine (TMB) in the presence of H_2O_2 to produce a blue color reaction. To examine the capability of CuS NPs as catalyst on the oxidation of TMB, 2.4 μL of 0.125 M TMB (dissolved in DMSO) in 3.0 ml acetate buffer (0.1 M and pH 4.0) was successively treated with (i) 20 μg CuS NPs, (ii) 2 μL of 30% H_2O_2, (iii) 2 μL of 30% H_2O_2 with 20 μg CuS NPs. All the reactions were monitored spectrophotometrically in time-scan mode at 653 nm. The kinetic analysis with TMB as the substrate was performed using 20 μg CuS NPs with fixed concentration of H_2O_2 (13 mM) and varying concentration of TMB (0, 8.3, 16.6, 29.1, 35.4, 41.6, 54.1, 62.5 and 75 μM). Similarly, the kinetic analysis with H_2O_2 as the substrate was performed using 20 μg CuS NPs with fixed concentration of TMB (100 μM) and varying concentrations of H_2O_2 (0, 6.5, 9.8, 13, 16, 19, 22.8, 26, 32 and 42 mM). Kinetic parameters were calculated based on the Michaelis–Menten:

$$V_0 = V_{\max}\frac{[S]}{[S]+K_M} \quad (1)$$

The Michaelis–Menten equation describes the relationship between the rates of substrate conversion by an enzyme and the concentration of the substrate. In this equation, V_0 is the rate of conversion, $V_{\max}$ is the maximum rate of conversion, [S] is the substrate concentration, and K_M is the Michaelis constant which is equivalent to the substrate concentration at which the rate of conversion is half of $V_{\max}$ and denotes the affinity of the enzyme for the substrate.

2.5. Glucose determination

Glucose determination was carried out as follows: at first, 20 μL of 20 mg/mL glucose oxidase (GOx) and 200 μL of D-glucose with different concentrations were mixed in 0.01 M phosphate buffer solution (PBS, pH 7.0) and incubated at 40 °C for 40 min; then 2.4 μL of 0.125 M TMB, 20 μL of 5 mg/mL CuS NPs and 2 mL of 0.1 M acetate buffer (pH 4.0) were successively added into the above 220 μL GOx–glucose reaction system; finally the mixed solution was incubated at 40 °C for 15 min for the absorption spectroscopy measurement.

In order to investigate the mechanism of the glucose catalytic reaction, where hydroxyl radical may be produced from the decomposition of H_2O_2, the commonly used terephthalic acid (TA) photoluminescence probing technique [50] was adopted. In this experiment, 2×10^{-3} M sodium terephthalate, 0.045 M glucose, 3 mL of 20 mg/mL GOx in aqueous PBS (0.01 M, pH 7.0) and two different amounts (0 and 20 mg) of CuS NPs were incubated at 40 °C for 10 h. Then the luminescence spectrum was measured between 330 and 540 nm using 315 nm as the excitation wavelength.

2.6. Determination of Blood glucose using CuS NPs

For glucose determination in blood from healthy human volunteers, the collected sample was stored in freeze and then was centrifuged at 12,000 rpm for 40 min. After that, the supernatant solution was diluted 24 times using PBS (0.01 M, pH 7.0) before subsequent use. This diluted serum was then used with GOx for glucose catalyzed reaction as stated above instead of glucose aqueous solution and the corresponding absorbance was measured at a wavelength of 653 nm.

3. Results and discussion

3.1. Synthesis and characterization of CuS NPs

CuS NPs was synthesized from Cu(II) precursor complex of pyridine-2-carboxamide as copper source in the presence of excess pyridine-2-carboxamide which itself acts as capping agent (Scheme 1). Herein, water is selected as solvent, but no commercial capping agent or additive is involved in this method.

The crystallinity and phase purities of CuS NPs were first examined by the X-ray diffraction (XRD) technique. The diffraction patterns of the crystalline products match quite well with the standard diffraction data of the pure primitive hexagonal phase of the covellite structure of CuS (JCPDS no. 78-2121) with $P6_3/mmc$ space group and hexagonal primitive unit cell with $a=b=3.791$ and $c=16.34$ Å. In Fig. 1, the peaks at 2θ values of 29.20, 31.85, 32.76, 47.90 and 59.34 can be indexed to the (102), (103), (006), (110) and (116) planes of CuS, respectively. Any other characteristic peaks of impurities, such as $Cu_{1.8}S$, $Cu_{1.96}S$, Cu_2S or CuO, were not detected. The relative broad feature of the peaks (FWHM) indicates the presence of smaller crystallites. The average size of the CuS nanoparticles was estimated from the diffraction peak (110) by using the Debye-Scherrer equation ($D=0.9\lambda/(\beta\mathrm{Cos}\theta)$) as about 30 nm, where D is the crystallite diameter, λ is the wavelength of X-ray, i.e. 1.540598 Å, β is the value of full width at half maximum and θ is the Bragg's angle.

The size and morphology of the product were analyzed by transmission electron microscopy (TEM). Typical TEM image in Fig. 2a illustrates that the CuS NPs are composed of rectangular or quasi-rectangular nanoparticles with average diameter of 40–50 nm. Selected area electron diffraction (SAED) pattern of the CuS NPs (Fig. 2b) exhibits a set of concentric rings that can be indexed to (102), (006), (110), and (116) diffraction planes for hexagonal phase of CuS. These findings are consistent with the observations made from the XRD patterns. Fig. 2c shows the HRTEM image of CuS NPs, which displays clear image of lattice fringes of the prepared nanocrystals, indicating the good crystalline nature of CuS NPs. The interplanar spacing is about 0.281 nm corresponding to the (103) lattice plane of hexagonal CuS. In addition, the corresponding fast fourier transform (Live FFT) image (Fig. 2d) also supports the single-crystalline nature of the CuS NPs with the assigned crystal planes of (102).

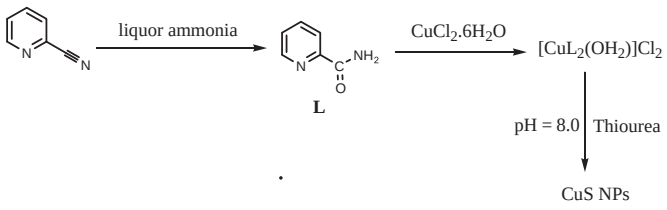

Scheme 1. Preparation of CuS nanoparticles.

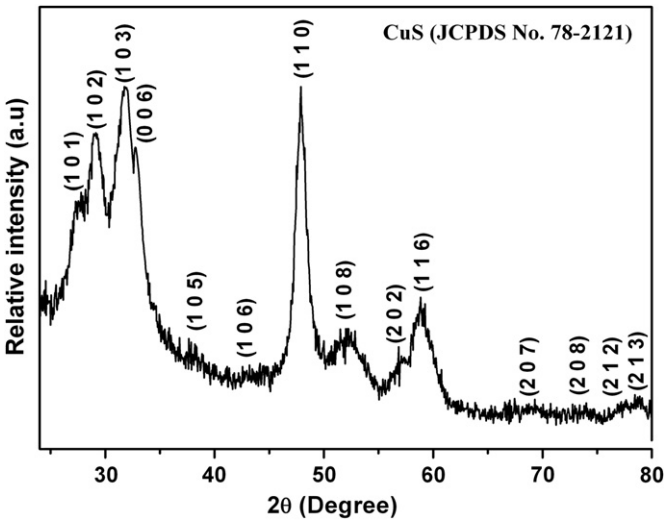

Fig. 1. Powder XRD pattern of CuS NPs.

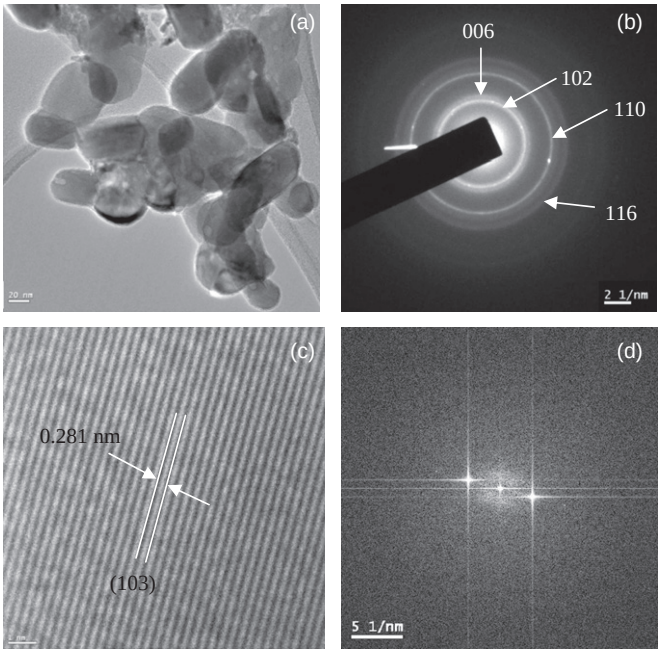

Fig. 2. (a) TEM, (b) SAED pattern, (c) HRTEM and (d) Live FFT image of CuS NP.

The optical absorption spectrum (Fig. S1) of the blackish-green CuS NPs also supports the formation of covellite phase [51,52] and the band gap energy is calculated as 2.09 eV which is also consistent with CuS covellite phase formation. The surface area of the NPs was investigated as 29.7 $m^2\,g^{-1}$ through Brunauer–Emmett–Teller (BET) analysis at 77 K (Fig. S2).

3.2. Peroxidase-like activity of the CuS NPs

The peroxidase-like activity of the as-prepared CuS NPs was tested through the catalytic oxidation of a peroxidase substrate, TMB in the presence of H_2O_2. TMB has been proved to be a non-carcinogenic derivative [53] and can be oxidized to a blue reaction product (Fig. 3a inset) in the presence of H_2O_2. The catalytic reaction can be monitored spectrophotometrically at room temperature from augmentation of TMB absorbance [19] at 653 nm (Fig. 3b), which is originated from the oxidation product of TMB similar to the phenomenon observed for the commonly used horseradish peroxidase (HRP) [19]. These phenomena indicate that the CuS nanostructure indeed exhibits peroxidase-like efficiency. The enzyme like activity of the CuS NPs may originate from the Cu^{2+} ions present at the surface of the NPs. Similar to Fe^{3+} or Fe^{3+} [49] this Cu^{2+} ion may acts as Fenton-like reagent and interact with the substrate in presence of hydrogen peroxide, resulting in a colored reaction product. The mechanism most likely follows Fenton's reaction [54] and can be written as follows:

$$Cu^{2+} + H_2O_2 \rightarrow Cu^{1+} + HOO^{\bullet} + H^{+} \quad (2)$$

$$Cu^{1+} + H_2O_2 \rightarrow Cu^{2+} + {}^{\bullet}OH + OH^{-} \quad (3)$$

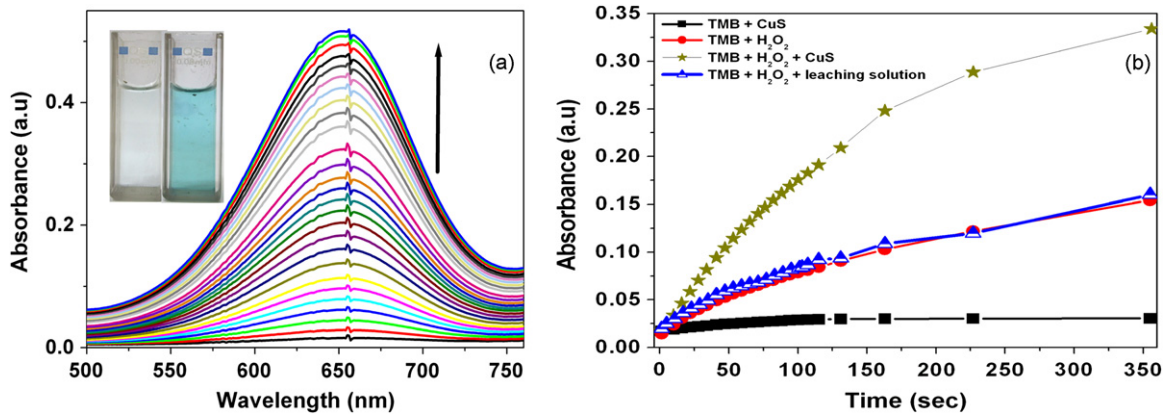

Fig. 3. (a) Time dependent UV–Vis spectral changes of TMB–H_2O_2 system catalyzed by CuS NPs. Inset: Typical photography of TMB reaction system (from left to right: with only catalyst nanoparticles (colorless), with H_2O_2 after catalytic reaction by nanoparticles (blue color). (b) UV–Vis absorption-time course curve of TMB under different conditions.

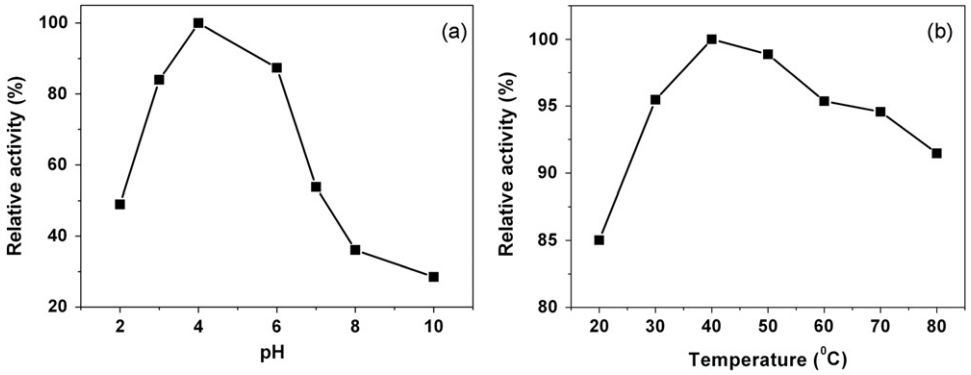

Fig. 4. Effects of (a) pH and (b) temperature on the catalytic oxidation of TMB in the presence of CuS NPs.

The hydroxyl radical, formed in the course of reaction, may catalyze the oxidation of the TMB substrate, resulting in a blue colored product.

Additional control experiments showed that the absorbance at 653 of the CuS–TMB–H_2O_2 (Fig. 3b) system was much higher than that of the TMB–H_2O_2 (Fig. 3b) system over 350 s run, and the CuS–TMB (Fig. 3b) system had no absorbance in 653 nm. It indicated that both the components were required for the reaction, as was also the case for horseradish peroxidase (HRP). The results also confirmed that the CuS NPs exhibits an intrinsic peroxidase-like activity.

It is important to rule out the possibility that the observed peroxidase-like catalytic activity is caused by copper ions leaching from CuS NPs in the solution. To test this, leaching solution was obtained by incubating CuS NPs in the reaction buffer (pH 4.0) for 1 h and then CuS NPs were removed from solution by centrifugation. As shown in Fig. 3b, change of absorbance at 653 nm was same as that of TMB–H_2O_2 system. These observations clearly indicate that there is no marked change in the absorbance when the leaching solution was used instead of CuS NPs under the same reaction conditions. These experimental results also reveal that the observed peroxidase-like activity can be attributed to intact nanoparticles.

Similar to NPs based peroxidase mimetics and HRP, the catalytic activity of CuS NPs is dependent on pH and temperature. To find out the optimum pH and temperature, at first we have examined the effects of pH and temperature on the catalytic oxidation of TMB in the presence of CuS NPs between the pH range 2.0–8.0 and the temperature range 10–80 °C, respectively. Fig. 4 demonstrates that CuS NPs exhibits higher catalytic efficiency in acidic condition than that in neutral or basic conditions. Hence, the pH 4.0 and 40 °C were chosen as the optimum pH and temperature (Fig. 4), which are very similar to the values for HRP [19].

To investigate the kinetic mechanism of the peroxidase catalytic activity of CuS NPs, The steady-state kinetic assays were carried out at room temperature under the optimum conditions, 0.1 M NaOAc, pH 4.0 and 40 °C. The kinetic parameters for the reaction were evaluated by the initial rate method i.e. calculating the slopes of initial absorbance changes with time. To investigate the apparent steady-state reaction rates, time-scan was started as quickly as possible and the absorbance variation with time was continuously monitored at 653 nm. The absorbance data were converted to corresponding concentration terms by using the value $\varepsilon = 39000\ M^{-1}cm^{-1}$ (at 653 nm) for the oxidized product of TMB [55]. During the kinetic analysis, experiments were performed with fixed concentration of H_2O_2 and varying concentration of TMB or vice versa in the presence of CuS NPs. It is found that over a suitable range of TMB (Fig. 5a) and H_2O_2 (Fig. 5b) concentrations, the plots of initial rate vs. TMB or H_2O_2 concentration, show typical Michaelis–Menten like behavior.

The data were fitted to the Michaelis–Menten model using a non-linear least square fitting routine to obtain the catalytic parameters [Michaelis–Menten constant (K_m^{app}) =0.0072 mM and maximum initial velocity (V_{max})=8.96×10^{-8} M S^{-1} with TMB as the substrate. On the other hand, the K_m^{app} and V_{max} of CuS NPs with H_2O_2 as the substrate are 12.0 mM and 2.09×10^{-7} M S^{-1}, respectively. All these parameters were also evaluated from the Lineweaver–Burk [56] double-reciprocal plot ($1/V_0$ vs. $1/S_0$), which gave analogous values (Fig. 5a and b insets). From these catalytic parameters, we can conclude that our as-synthesized CuS NPs

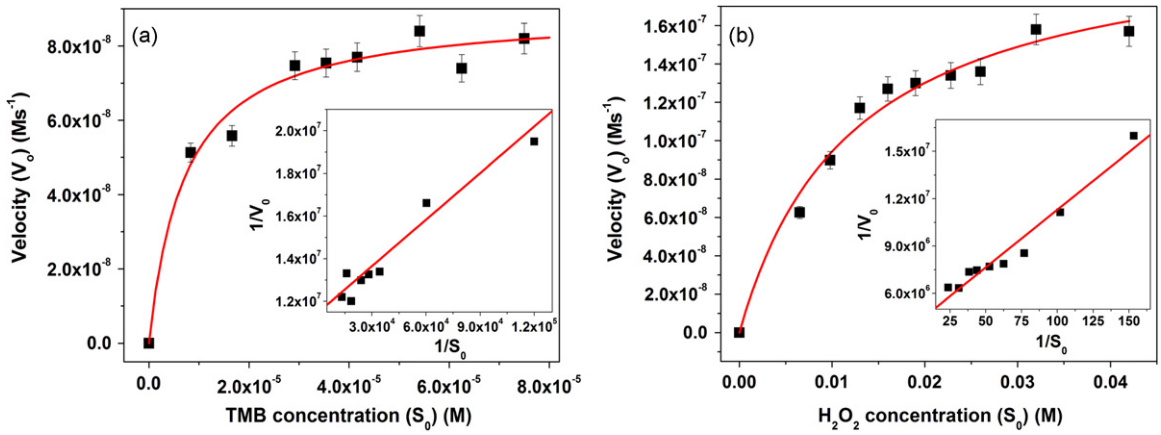

Fig. 5. Steady-state kinetic analyses using the Michaelis–Menten model and Lineweaver–Burk model (insets) for CuS NPs by (a) varying the concentration of TMB with fixed amount of H_2O_2 and (b) varying the concentration of H_2O_2 with fixed amount of TMB.

possessed intrinsic peroxidase-like activity and good affinity for both TMB and H_2O_2. Hence it can be used as artificial peroxidase-mimic.

3.3. Analytical application in determination of glucose

On the basis of the inherent peroxidase property of the CuS NPs, we designed a colorimetric method for detection of glucose by utilizing the same chromogenic substrate TMB and TMB–H_2O_2 catalysized color reaction studied above. When the above TMB–H_2O_2 catalytic reaction is coupled with the glucose catalytic reaction by GOx, the colorimetric detection of glucose could be eagerly understood because H_2O_2 is the main product of the GOx-catalyzed reaction. Generally, glucose oxidase catalyzed the oxidation of glucose to produce gluconic acid and hydrogen peroxide in the presence of oxygen. Subsequently, the formed hydrogen peroxide was catalyzed by CuS NPs and then reacted with TMB, resulting in the development of a blue color. Therefore, the color change from the converted TMB was employed to indirectly measure glucose content. As the GOx denatured in pH 4.0, the glucose detection was performed in two steps: in the first step, the glucose oxidation reaction with GOx was performed in pH 7.0 buffer solutions to produce H_2O_2 while in the second step this H_2O_2 was reduced by TMB co-substrate in presence of CuS NPs at pH 4.0. Fig. 6 illustrates a typical absorbance (653 nm) versus glucose concentration response plot of the sensor in the detection of glucose where the response is linear in the glucose concentration range 2–1800 μM with a detection limit of 0.12 μM. Compared with several previously reported glucose sensors [8,10,22,42,57–62] (Table 1), the CuS NPs shows either comparable or even better response towards glucose.

3.4. Mechanism of the reactions involve in glucose determination process

The nature of glucose catalytic reaction may originate from the generation of hydroxyl radical (OH•) from the decomposition of H_2O_2. The sequences of reactions that seem to be involved in the colorimetric glucose determination technique are summarized below:

$$O_2 + \text{Glucose} \xrightarrow{GO_X} H_2O_2 + \text{Gluconic acid} \quad (4)$$

$$H_2O_2 \xrightarrow{CuS} OH\bullet \quad (5)$$

$$\text{TMB(colorless)} + OH\bullet \xrightarrow{CuS} \text{oxidised TMB(blue)} + H_2O \quad (6)$$

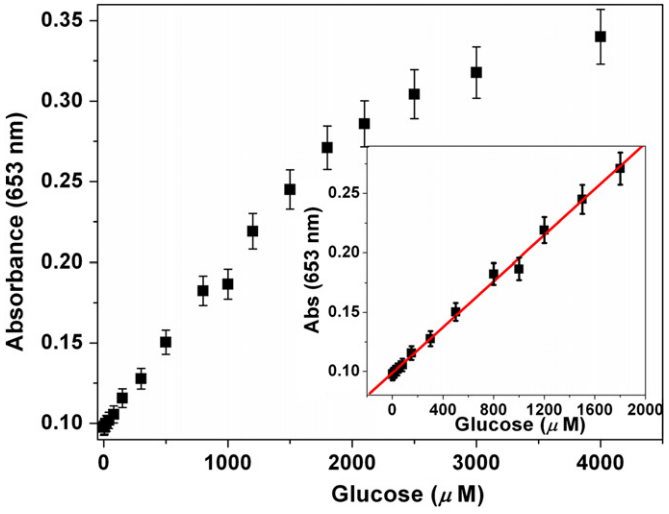

Fig. 6. Glucose concentration-response curve for colorimetric determination of glucose using GOx/TMB/CuS system. Concentration of TMB: 4.5×10^{-3} M; CuS NPs: 20 μL of 5 mg/mL. Inset: corresponding linear calibration plot.

In the first step, glucose is oxidized by molecular oxygen in presence of glucose oxidase (GOx) Eq. (4). The H_2O_2, thus produced, then gets adsorbed over CuS NPs surface and then activated by the bound Cu^{2+} to generate the OH• radical viz the Fenton-type reaction [54] Eq. (5). The generated OH• was stabilized by CuS via partial electron exchange interactions [63]. The OH• then quantitatively oxidize TMB to corresponding blue colored oxidized product according to Eq. (6).

The formation of OH• was confirmed by terephthalic acid (TA) photoluminescence probing techniques [50], which is highly sensitive and selective method, widely used in detection of hydroxyl radical. In presence of glucose reacting system, non-luminescent terephthalic acid (TA) easily reacted with OH• and is converted to highly fluorescent 2-hydroxy terephthalic acid (HTA) [64] according to Eq. (7).

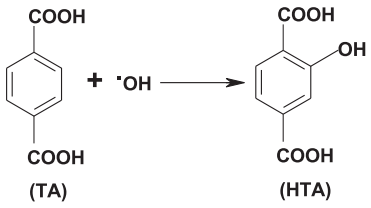

(7)

Table 1
Comparison of colorimetric glucose response parameters for CuS NPs with other glucose sensors.

Catalyst	Linear range (μM)	Detection limit (μM)	Reference
CuS NPs	2–1800	0.12	This work
Fe_3O_4 nanoparticles	50–1000	30	[8]
Carboxyl-modified graphene oxide	1–20	1	[10]
CuO	100–8000	–	[22]
Gold nanoparticles	18–1100	4	[43]
Graphene oxide–Fe_3O_4	2–200	0.74	[57]
FeSe film	2–30	0.5	[58]
CoFe layered double hydroxide (CoFe-LDHs) nanoplates	1–10	0.6	[59]
AuNPs (H_2O_2 triggered sol–gel transition)	0–131	1	[60]
Chitosan stabilized silver nanoparticles (Ch–Ag NPs)	5–200	0.1	[61]
PB–Fe_2O_3 nanoparticles	1–80	0.16	[62]

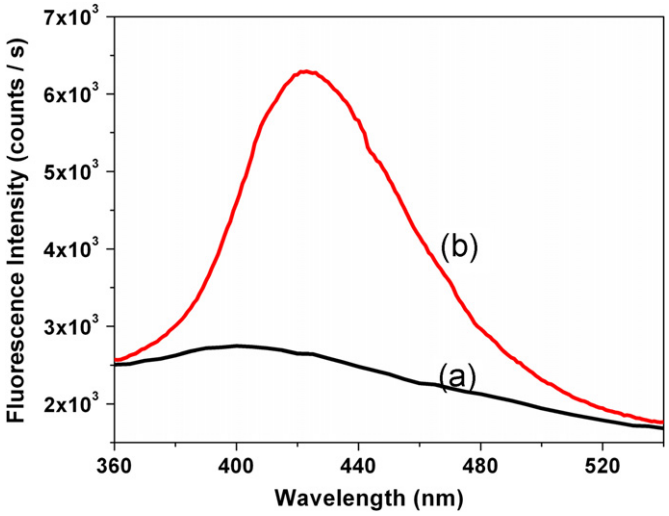

Fig. 7. Fluorescence spectral changes of sodium terephthalate solution (2×10^{-3} M) in the presence of fixed amount of glucose–GOx system and different amount of CuS catalyst, (a) 0 mg, (b) 20 mg during photoluminescence probing technique.

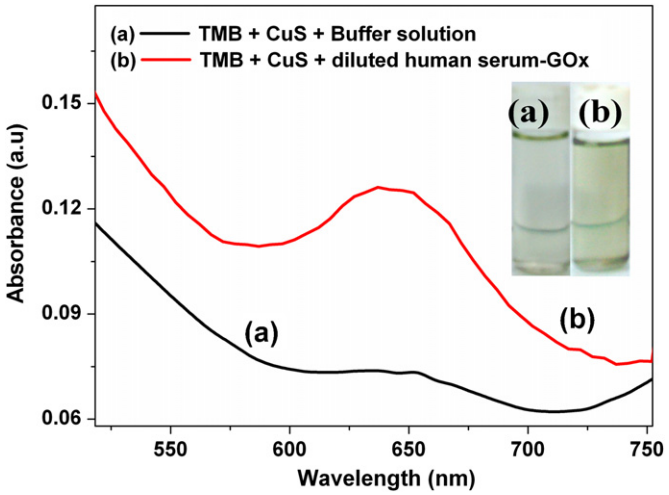

Fig. 8. UV–Vis spectra of buffer solution containing (a) TMB/CuS system and (b) TMB/CuS/diluted human serum–GOx system. Inset: images of corresponding colored product.

The photoluminescence spectra of Glucose–GOx/TA system without and with CuS NPs are displayed in Fig. 7, where the fluoresence intensity of the solution is increased dramatically with the addition of the CuS NPs. This phenomenon suggests that CuS NPs could decompose in situ formation of H_2O_2 from Glucose/GOx system to generate the $^{\bullet}OH$ radical.

3.5. Determination of human blood glucose using CuS NPs

Using the above glucose determination technique, we can detect and estimate glucose in real samples such as diluted serum of healthy human volunteers. Fig. 8 shows that after addition of diluted human serum, there occurs considerable change in color as well as UV–Vis spectra of TMB. According to the calibration curve, the concentration of glucose in the normal human serum sample is 6.05 mM (109.0 mg/dl) which is consistent with that measured through standard GOD–POD method in a pathological laboratory [6.27 mM (113.0 mg/dl)]. The general range of blood glucose concentration in healthy and diabetic persons is about 3–8 mM and 9–40 mM, respectively [65]. With the help of this simple colorimetric method we can monitor glucose level in diabetes patients.

4. Conclusion

In summary, CuS NPs were prepared by simple and green method and investigated as peroxidase mimetics. The catalytic oxidation of peroxidase substrate TMB with H_2O_2 using the CuS NPs was thoroughly studied. The CuS NPs as peroxidase mimetics provide a colorimetric assay for H_2O_2. More importantly, a sensitive and selective analytical platform for glucose detection was fabricated using glucose oxidase (GOx) and the as-prepared CuS NPs. The analytical platform developed exhibited sensitive and selective detection of glucose with a linear range from 2 to 1800 μM. As a novel mimic peroxidase, the CuS NPs demonstrate several advantages over HRP and other peroxidase nano-mimetics, such as stability, dispersibility, non-toxicity and high catalytic efficiency. On the basis of this finding, we provide a simple, inexpensive, highly sensitive, and selective method for colorimetric detection of blood glucose.

Acknowledgements

A.K. Dutta is indebted to UGC, India, for his senior research fellowship (SRF) [11-2/2002 (SA-I)]. S.D and S.S. is also thankful to CSIR, India, for their JRF [08/003(0072)/2010-EMR-I] and [08/003(0083)/2011-EMR-I]. P.B acknowledges DST, India for Fast Track Project (No. SR/FT/CS-022/2009) and CSIR [01(2459)/11/EMR-II] for financial support. The authors also acknowledge the facility developed in the Department of Chemistry, BESUS through MHRD (India) and UGC-SAP (India).

Appendix A. Supporting information

Supplementary data associated with this article can be found in the online version at http://dx.doi.org/10.1016/j.talanta.2013.01.032.

References

[1] L.C. Clark, C. Lyons, Ann. N.Y. Acad. Sci. 102 (1962) 29–45.
[2] V. Sanz, S. de Marcos, J.R. Castillo, J. Galban, J. Am. Chem. Soc. 127 (2005) 1038–1048.
[3] S. Lee, V.H. Perez-Luna, Anal. Chem. 77 (2005) 7204–7211.
[4] Y. Jiang, H. Zhao, Y.Q. Lin, N.N. Zhu, Y.R. Ma, L.Q. Mao, Angew. Chem. Int. Ed. 49 (2010) 4800–4804.
[5] C. Radhakumary, K. Sreenivasan, Anal. Chem. 83 (2011) 2829–2833.
[6] R.J. Russell, M.V. Pishko, C.C. Gefrides, M.J. McShane, G.L. Cote, Anal. Chem. 71 (1999) 3126–3132.
[7] Z.G. Wang, O.I. Wilner, I. Willner, Nano Lett. 9 (2009) 4098–4102.
[8] H. Wei, E. Wang, Anal. Chem. 80 (2008) 2250–2254.
[9] Y.J. Song, X.H. Wang, C. Zhao, K.G. Qu, J.S. Ren, X.G. Qu, Chem. Eur. J. 16 (2010) 3617–3621.
[10] Y.J. Song, K.G. Qu, C. Zhao, J.S. Ren, X.G. Qu, Adv. Mater. 22 (2010) 2206–2210.
[11] Y. Jv, B.X. Li, R. Cao, Chem. Commun. 46 (2010) 8017–8019.
[12] Y.J. Song, W.L. Wei, X.G. Qu, Adv. Mater. 23 (2011) 4215–4236.
[13] G. Zhang, P.K. Dasgupta, Anal. Chem. 64 (1992) 517–522.
[14] Q.G. Wang, Z.M. Yang, M.L. Ma, C.K. Chang, B. Xu, Chem. Eur. J. 14 (2008) 5073–5078.
[15] Y.Q. Xi, H.O. Qiu, M. Yang, H.S. Zhuang, Chin. J. Anal. Chem. 36 (2008) 1343–1348.
[16] R.P. Bonarlaw, J.K.M. Sanders, J. Am. Chem. Soc. 117 (1995) 259–271.
[17] Z.H. Liu, R.X. Cai, L.Y. Mao, H.P. Huang, W.H. Ma, Analyst 124 (1999) 173–176.
[18] L.G. Marinescu, M. Bols, Angew. Chem. Int. Ed. 45 (2006) 4590–4593.
[19] L. Gao, J. Zhuang, L. Nie, J.B. Zhang, Y. Zhang, N. Gu, T.H. Wang, J. Feng, D.L. Yang, S. Perrett, X.Y. Yan, Nat. Nanotechnol. 2 (2007) 577–583.
[20] A. Asati, S. Santra, C. Kaittanis, S. Nath, J.M. Perez, Angew. Chem., Int. Ed. 48 (2009) 2308–2312.
[21] W. Chen, J. Chen, A.L. Liu, L.M. Wang, G.W. Li, X.H. Lin, Chem. Cat. Chem 3 (2011) 1151–1154.
[22] W. Chen, J. Chen, Y.B. Feng, L. Hong, Q.Y. Chen, L.F. Wu, X.H. Lina, X.H. Xia, Analyst 137 (2012) 1706–1712.
[23] J. Mu, Y. Wang, M. Zhao, L. Zhang, Chem. Commun. 48 (2012) 2540–2542.
[24] R. Andre, F. Natalio, M. Humanes, J. Leppin, K. Heinze, R. Wever, H.C. Schroeder, W.E.G. Mueller, W. Tremel, Adv. Funct. Mater. 21 (2011) 501–509.
[25] W. Luo, Y.S. Li, J. Yuan, L. Zhu, Z. Liu, H. Tang, S. Liu, Talanta 81 (2010) 901–907.
[26] W. Shi, X. Zhang, S. He, Y. Huang, Chem. Commun. 47 (2011) 10785–10787.
[27] Z. Dai, S. Liu, J.H. Ju, Chem. Eur. J. 15 (2009) 4321–4326.
[28] S.K. Maji, A.K. Dutta, P. Biswas, D.N. Srivastava, P. Paul, A. Mondal, B. Adhikary, Appl. Catal. A Gen. 419 (2012) 170–177.
[29] S.K. Maji, A.K. Dutta, D.N. Srivastava, P. Paul, A. Mondal, B. Adhikary, J. Mol. Catal. A Chem. 358 (2012) 1–9.
[30] A.K. Dutta, S.K. Maji, D.N. Srivastava, A. Mondal, P. Biswas, P. Paul, B. Adhikary, ACS Appl. Mater. Interfaces 4 (2012) 1919–1927.
[31] R.J. Cui, Z.D. Han, J.J. Zhu, Chem. Eur. J 17 (2011) 9377–9384.
[32] W.B. Shi, Q.L. Wang, Y.J. Long, Z.L. Cheng, S.H. Chen, H.Z. Zheng, Y.M. Huang, Chem. Commun. 47 (2011) 6695–6697.
[33] N. Ding, N. Yan, C. Ren, X. Chen, Anal. Chem. 82 (2010) 5897–5899.
[34] M. Basu, A.K. Sinha, M. Pradhan, S. Sarkar, Y. Negishi, P.T. Govind, Environ. Sci. Technol. 44 (2010) 6313–6318.
[35] J.G. Yu, J. Zhang, S. Liu, J. Phys. Chem. C 114 (2010) 13642–13649.
[36] A.B.F. Martinson, J.W. Elam, M.J. Pellin, Appl. Phys. Lett. 94 (2009) 123107–123110.
[37] J. Gao, Q. Li, H. Zhao, L. Li, C. Liu, Q. Gong, L. Qi, Chem. Mater. 20 (2008) 6263–6269.
[38] J. Liu, D. Xue, J. Mater Chem. 21 (2011) 223–228.
[39] J.S. Chunga, H.J. Sohn, J. Power Sources 108 (2002) 226–231.
[40] J. Lu, R.F. Bu, Z.L. Sun, Q.S. Lu, H. Jin, Y. Wang, S.H. Wang, L. Li, Z.L. Xie, B.Q. Yang, Diabetes Res. Clin. Pract. 93 (2011) 179–186.
[41] J. Wang, K.S. Carmon, L.A. Luck, I.I. Suni, Electrochem. Solid State Lett. 8 (2005) H61–H64.
[42] E.S. Forzani, H.Q. Zhang, L.A. Nagahara, I. Amlani, R. Tsui, N. Tao, Nano Lett. 4 (2004) 1785–1788.
[43] R. Gill, L. Bahshi, R. Freeman, I. Willner, Angew. Chem. Int. Ed. 47 (2008) 1676–1683.
[44] V. Sanz, S.D. Marcos, J.R. Castillo, J. Galban, J. Am. Chem. Soc. 127 (2005) 1033–1038.
[45] R. Kurita, H. Tabei, Y. Iwasaki, K. Hayashi, K. Sunagawa, O. Niwa, Biosens. Bioelectron. 20 (2004) 518–523.
[46] P.F. Pang, Y.L. Zhang, S.T. Ge, Q.Y. Cai, S.Z. Yao, C.A. Grimes, Sens. Actuators B 136 (2009) 310–314.
[47] H.S.M. Abd-Rabboh, M.E. Meyerhoff, Talanta 72 (2007) 1129–1133.
[48] S. Cosnier, F. Lambert, M. Stoytcheva, Electroanalysis 12 (2000) 356–360.
[49] W. He, H. Jia, X. Li, Y. Lei, J. Li, H. Zhao, L. Mi, L. Zhang, Z. Zheng, Nanoscale 4 (2012) 3501–3506.
[50] J.C. Barreto, G.S. Smith, N.H.P. Strobel, P.A. McQuillin, T.A. Miller, Life Sci. 56 (1995) 89–96.
[51] P. Roy, S.K. Srivastava, Crys. Growth Des. 6 (2006) 1921–1926.
[52] T.Itoh Kuzuya, K. Ichidate, M. Wakamatsu, Y. Fukunaka, K. Sumiyama, Electrochim. Acta 53 (2007) 213–217.
[53] S. Savard, P.D. Josephy, Mutagenesis 2 (1987) 97–105.
[54] W.P. Kwan, B.M. Volker, Environ. Sci. Technol. 37 (2003) 1150–1158.
[55] E.I. Karaseva, Y.P. Losev, D.I. Metelitsa, Russ. J. Bioorg. Chem. 28 (2002) 128–135.
[56] L. Lineweaver, D. Burk, J. Am. Chem. Soc. 56 (1934) 658–666.
[57] Y. Dong, H. Zhang, Z.U. Rahman, L. Su, X. Chen, J. Hu, X. Chen, Nanoscale 4 (2012) 3969–3976.
[58] A.K. Dutta, S.K. Maji, A. Mondal, B. Karmakar, P. Biswas, B. Adhikary, Sens. Actuators B Chem. 173 (2012) 724–731.
[59] Y. Zhang, J. Tian, S. Liu, L. Wang, X. Qin, W. Lu, G. Chang, Y. Luo, A.M. Asiri, A.O. Al-Youbi, X. Sun, Analyst 137 (2012) 1325–1328.
[60] C. Xu, J. Ren, L. Feng, X. Qu, Chem. Commun. 48 (2012) 3739–3741.
[61] H. Jiang, Z. Chen, H. Cao, Y. Huang, Analyst 137 (2012) 5560–5564.
[62] A.K. Dutta, S.K. Maji, P. Biswas, B. Adhikary, Sens. Actuators B Chem. 177 (2013) 676–683.
[63] W. Shi, X. Zhang, S. He, Y. Huang, Chem. Commun. 47 (2011) 10785–10787.
[64] K. Ishibashi, A. Fujishima, T. Watanabe, K.J. Hashimoto, Photochem. Photobiol. A 134 (2000) 139–142.
[65] Y. Xu, P.E. Pehrsson, L. Chen, R. Zhang, W.J. Zhao, Phys. Chem. C 111 (2007) 8638–8643.